Available online at www.sciencedirect.com

SCIENCE DIRECT®

Polymer 46 (2005) 2424–2432

polymer

www.elsevier.com/locate/polymer

Optically active photochromic methacrylic polymers with controlled average molecular weight and defined end-groups by atom transfer radical polymerization

L. Angiolini*, T. Benelli, L. Giorgini, E. Salatelli

Dipartimento di Chimica Industriale e dei Materiali and INSTM UdR-Bologna, University of Bologna, Viale Risorgimento 4, 40136 Bologna, Italy

Received 20 January 2005; received in revised form 9 February 2005; accepted 11 February 2005

Abstract

We report a new approach based on atom transfer radical polymerization (ATRP) to produce optically active polymers containing azoaromatic moieties in the side chain with controlled average molecular weights, that can be used to investigate the conformational origin of chirality in this class of synthetic materials. The ATRP technique has been successfully applied to the synthesis of a series of optically active photochromic homopolymers poly[(*S*)-3-methacryloyloxy-1-(4-azobenzene)pyrrolidine] {poly[(*S*)-**MAP**]}, containing a chiral group of one prevailing configuration interposed between the methacrylic moiety and the photochromic azoaromatic chromophore. By just changing the duration of the polymerization process, macromolecules having distinct average chain lengths with low polydispersity values and well defined end-groups have been obtained.

Optical activity and thermal properties of the resulting polymeric derivatives result to depend on their average molecular weight. In particular, a dependence of optical rotation and circular dichroism on chain-length has been evidenced.

Keywords: Atom transfer radical polymerization; Photochromic chiral polymers; Azobenzene-containing polymers

1. Introduction

In previous studies [1–3] we reported the synthesis of a new class of optically active photochromic methacrylic polymers bearing in the side chain both a chiral group of one single configuration and the *trans*-azoaromatic moiety with a conjugated electron donor–acceptor system. This functional combination allows the polymers to display both the properties typical of dissymmetric systems [4] (optical activity, absorption of circularly polarized light in the UV–Vis spectral region), as well as the features of photochromic materials (NLO properties, photoresponsiveness, photorefractivity) [5,6]. Thus, these materials are considered of remarkable interest for several advanced technological applications, such as optical storage, waveguides, chiroptical switches, etc. [7–10].

With the aim to investigate the dependence of the physico-chemical properties of these macromolecules on their average molecular weight, in the present paper, for the first time, atom transfer radical polymerization (ATRP) [11] has been used to obtain a series of the above optically active methacrylic homopolymers of different chain length. ATRP is one of the most successful methods for the synthesis of macromolecules with controlled molecular weight and molecular weight distribution. It is in fact very versatile, being suitable to polymerize a wide range of monomers, insensitive to many functional groups and tolerant towards impurities present in solvent and reactants, including water. Several methacrylic esters have been successfully polymerized with this method, for example *n*-butyl methacrylate [12–14], fluorinated methacrylic esters [15,16] and 1-phenoxycarbonyl ethyl methacrylate [17], as well as liquid crystalline polymers containing azoaromatic moieties in the side-chain [18–20].

The ATRP process is based on a transition metal halide/nitrogen based ligand catalyst [21,22] and has been adopted for the preparation of a series of polymeric derivatives (poly-1 through poly-6), starting from the

---

* Corresponding author. Tel./fax: +39 051 2093687.
E-mail address: luigi.angiolini@unibo.it (L. Angiolini).

0032-3861/$ - see front matter © 2005 Published by Elsevier Ltd.
doi:10.1016/j.polymer.2005.02.023

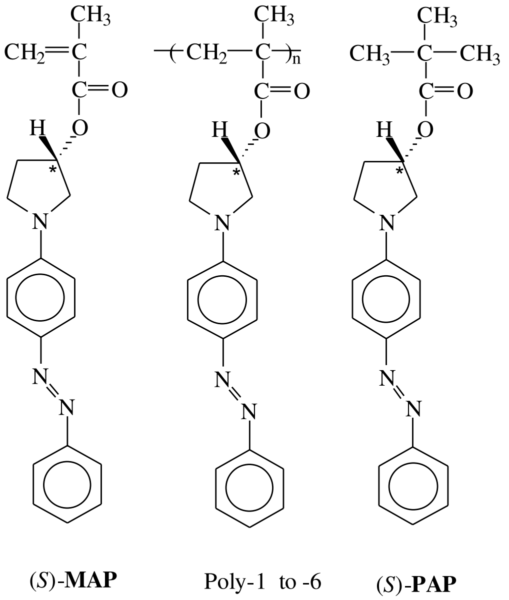

Fig. 1. Chemical structures of monomer, homopolymers and model compound.

corresponding monomer (*S*)-3-methacryloyloxy-1-(4-azobenzene)pyrrolidine [(*S*)-**MAP**] bearing a cyclic pyrrolidine group of one single configuration and the *trans*-azoaromatic chromophore (Fig. 1).

In particular we have used allyl 2-bromoisobutyrate (**ABIB**) as the initiator of radical living polymerization and the transition metal salt Cu(I)Br, in combination with 1,1,4,7,10,10-hexamethyltriethylenetetramine (**HMTETA**) as ligand [23]. This method has allowed us to obtain macromolecules having various average chain lengths and sufficiently low polydispersity values just by changing the process duration.

Optical activity, electronic spectra and thermal properties of the products obtained by ATRP, have been compared with those displayed by poly[(*S*)-3-methacryloyloxy-1-(4-azobenzene)pyrrolidine], poly[(*S*)-**MAP**], previously obtained by AIBN-initiated polymerization [1], as well as with the low molecular weight model compound (*S*)-(+)-3-pivaloyloxy-1-(4-azobenzene)pyrrolidine [(*S*)-**PAP**] [1] (Fig. 1), representative of the repeating unit of polymeric derivatives, thus achieving indications about the effects originated in the system by the progressive increase of chain length.

2. Experimental

2.1. Physico-chemical measurements

^{1}H- and ^{13}C-NMR spectra were obtained at room temperature, on 5–10% $CDCl_3$ solutions, using a Varian NMR Gemini 300 spectrometer. Chemical shifts are given in ppm from tetramethylsilane (TMS) as the internal reference. ^{1}H-NMR spectra were run at 300 MHz by using the following experimental conditions: 24,000 data points, 4.5 kHz spectral width, 2.6 s acquisition time, 128 transients. ^{13}C-NMR spectra were recorded at 75.5 MHz, under full proton decoupling, by using the following experimental conditions: 24,000 data points, 20 kHz spectral width, 0.6 s acquisition time, 64,000 transients. FT-IR spectra were carried out on a Perkin–Elmer 1750 spectrophotometer, equipped with an Epson Endeavour II data station, on samples prepared as KBr pellets.

UV–Vis absorption spectra were recorded at 25 °C in the 700–250 nm spectral region with a Perkin–Elmer Lambda 19 spectrophotometer on $CHCl_3$ solutions by using cell path lengths of 0.1 cm. Concentrations in azobenzene chromophore of about 3×10^{-4} mol L^{-1} were used.

Optical activity measurements were accomplished at 25°C on $CHCl_3$ solutions ($c\approx0.250$ g dL^{-1}) with a Perkin Elmer 341 digital polarimeter, equipped with a Toshiba sodium bulb, using a cell path length of 1 dm. Specific and molar rotation values at the sodium D line are expressed as deg dm^{-1} g^{-1} cm^{3} and deg dm^{-1} mol^{-1} dL, respectively.

Circular dichroism (CD) spectra were carried out at 25 °C on $CHCl_3$ solutions on a Jasco 810 A dichrograph, using the same path lengths and solution concentrations as for the UV-vis measurements. $\Delta\varepsilon$ values, expressed as L mol^{-1} cm^{-1} were calculated from the following expression: $\Delta\varepsilon=[\Theta]/3300$, where the molar ellipticity $[\Theta]$ in deg cm^{2} $dmol^{-1}$ refers to one azobenzene chromophore.

Number average molecular weights of the polymers ($\bar{M}_n$) and their polydispersity indexes ($\bar{M}_w/\bar{M}_n$) were determined in THF solution by SEC using a HPLC Lab Flow 2000 apparatus, equipped with an injector Rheodyne 7725i, a Phenomenex Phenogel 5-micron MXL or MXM column and a UV-VIS detector Linear Instrument model UVis-200, working at 254 nm. Calibration curves for MXL and MXM columns were obtained by using monodisperse polystyrene standards in the range 800–35,000 and 2,700–200,000, respectively.

The glass transition temperature values were determined by differential scanning calorimetry (DSC) on a TA Instrument DSC 2920 Modulated apparatus at a heating rate of 10 °C/min under nitrogen atmosphere on samples weighing 5–9 mgr. Check of the liquid crystalline behaviour was carried out with an Zeiss Axioscope2 polarising microscope through crossed polarizers fitted with a Linkam THMS 600 hot stage.

The initial thermal decomposition temperature (T_d) was determined on the polymeric samples with a Perkin–Elmer TGA-7 thermogravimetric analyzer by heating the samples in air at a rate of 20 °C/min.

2.2. Materials

The monomer (*S*)-(+)-3-methacryloyloxy-1-(4-azobenzene)pyrrolidine [(*S*)-**MAP**] and the model compound (*S*)-

(+)-3-pivaloyloxy-1-(4-azobenzene)pyrrolidine [(*S*)-**PAP**] were synthesized as previously reported [1].

Chloroform and THF were purified and dried according to the reported procedures [24] and stored under nitrogen.

Allyl 2-bromoisobutyrate (**ABIB**), 1,1,4,7,10,10-hexamethyltriethylenetetramine (**HMTETA**) and copper bromide were purchased from Aldrich and used as received.

2.3. Polymerization of (S)-MAP by ATRP

All the homopolymerizations of (*S*)-**MAP** were carried out in glass vials using **ABIB** as the initiator, **HMTETA** as the ligand, Cu(I)Br as catalyst and dry THF as solvent [(*S*)-**MAP**/THF 1/20 g/ml]. Several reaction mixtures [(*S*)-**MAP/ABIB/HMTETA**/CuBr =50:1:1:1 by mol] were introduced into the vials under nitrogen atmosphere, submitted to several freeze-thaw cycles and heated at 60 °C. To terminate the polymerization reaction, the vials were frozen after known reaction times, ranging from 2 to 24 h, with liquid nitrogen and the obtained polymers purified by precipitation in a large excess of methanol. The products (poly-1 through poly-6) were finally dried at 70 °C under vacuum for several days to constant weight.

Relevant data for the synthesized polymers are reported in Table 1. All the products were characterized by FT-IR, ^{1}H- and ^{13}C-NMR. As an example, the spectroscopic data for poly-2, obtained after 4 h of reaction, are here reported.

^{1}H-NMR ($CDCl_3$): 7.90 (m, 4H, arom 2′-H and *metha* to amino group), 7.35 (m, 3H, arom 3′-H and 4′-H), 6.40 (m, 2H, arom *ortho* to amino group), 5.85 (1H, $CH_2{=}C\mathit{H}\text{-}CH_2$-), 5.30–4.60 (m, 1H, 3-CH and 2H, $C\mathit{H}_2{=}CH–CH_2$–), 4.45 (2H, $CH_2{=}CH–C\mathit{H}_2$–), 3.70–3.00 (m, 4H, 2- and 5-CH_2), 2.30–1.40 (m, 4H, 4-CH_2 and main chain CH_2), 1.40–0.50 ppm (m, 3H, main chain CH_3 and 6H, –$C(CH_3)_2$–COO–).

^{13}C-NMR ($CDCl_3$): 177.1 (CO), 153.6, 149.8, 144.5 (arom *C*-N=N-*C* and *C*-N–CH_2), 132.6 ($CH_2{=}\mathit{C}H\text{-}CH_2$–), 130.2 (arom 4′-C), 129.6 (arom 3′-C), 125.8, 122.9 (arom 2′-C and 3-C), 118.9 ($\mathit{C}H_2{=}CH–CH_2$–), 112.2 (arom 2-C), 75.4 (CH–O), 66.0 ($CH_2{=}CH–\mathit{C}H_2$–), 59.3 (*C*-Br), 55.0 (main chain *C*H_2–C), 53.1 (CH–*C*H_2–N), 46.3 (CH_2–*C*H_2–N), 45.5 (main chain CH_2-*C*), 42.3 (*C*$(CH_3)_2$), 31.1 (CH–*C*H_2–CH_2), 23.4 (C(*C*$H_3)_2$), 19.9 and 17.4 ppm (main chain CH_3).

FT-IR (KBr): 3069 (ν_{CH}, arom), 2981, 2853 (ν_{CH}, aliph), 1729 (ν_{CO}, ester), 1603 and 1515 ($\nu_{C=C}$, arom), 1131 ($\nu_{C–O}$), 821 (δ_{CH}, 1,4-disubst. arom ring), 766 and 690 (δ_{CH}, monosubst. arom ring) cm^{-1}.

3. Results and discussion

3.1. Synthesis and characterization

The mechanism of ATRP of (*S*)-**MAP** (Scheme 1) involves the reversible halogen abstraction by Cu(I) from **ABIB** thus providing a radical species which can react with the monomer to start the process. The subsequent propagation is controlled by the low and stationary concentration of active species resulting from the dynamic equilibrium between active and dormant species catalyzed by the transition metal complex.

The occurrence of polymerization involving the methacrylic double bond was confirmed by FT-IR, showing the disappearance of the band at 1634 cm^{-1}, related to the stretching vibration of the double bond in the monomer, and the shift of the estereal carbonyl stretching frequency from 1709 cm^{-1} in the monomer to higher frequencies (1729 cm^{-1}) in the polymer, due to the reduced electron delocalization determined by the reaction of the methacrylic double bond.

Accordingly, in the ^{1}H-NMR spectra (Fig. 2(a)) of the sample obtained after 4 h of reaction (poly-2), the resonances at 5.60 and 6.10 ppm related to the vinylidenic protons of monomer (*S*)-**MAP**, are absent and the methyl resonances are shifted from about 1.95 ppm to higher field.

In addition, all the ^{1}H-NMR spectra display the resonances of the allyl protons signals of **ABIB** residue at

Table 1
Characterization data of polymeric derivatives

Sample	Reaction duration (h)	Monomer conversion[a] (%)	$\bar{M}_n$[b] (g/mol)	$\bar{M}_n$[c] (g/mol)	$\bar{M}_w/\bar{M}_n$[b]	T_g (°C)[d]
Poly-1	2	9.5	2,600	3,700	1.2	122
Poly-2	4	30.4	4,100	5,000	1.3	139
Poly-3	8	37.7	5,200	5,800	1.3	143
Poly-4	14	43.5	7,200	nd[e]	1.4	149
Poly-5	18	53.8	8,200	nd[e]	1.4	153
Poly-6	24	67.7	10,000	nd[e]	1.4	160
Poly[(*S*)-**MAP**][f]	72	69	31,500	–	1.6	169

[a] Calculated as g of polymer/g of monomer ×100.

[b] Determined by SEC in THF at 25 °C.

[c] Determined by ^{1}H-NMR in chloroform solution at 25 °C.

[d] Determined by DSC, heating rate of 10 °C/min under nitrogen atmosphere.

[e] Not determined due to low intensity of the end-groups signals.

[f] Obtained by free radical polymerization by using AIBN as thermal initiator [1].

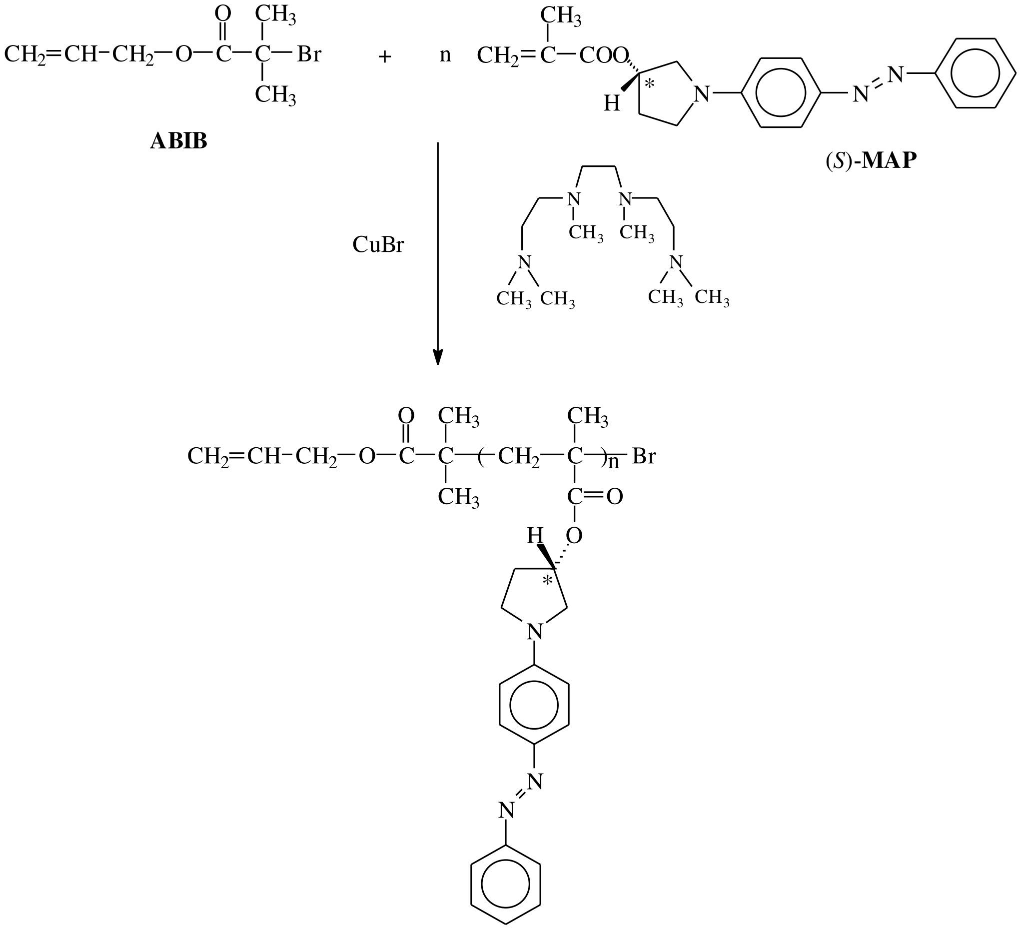

Scheme 1. ATRP of (*S*)-**MAP**.

4.45 ppm (2H, $CH_2{=}CH{-}CH_2{-}$) and 5.85 ppm (1H, $CH_2{=}CH{-}CH_2{-}$). These findings are confirmed by ^{13}C-NMR spectra (Fig. 2(b)): for example, poly-2 shows small signals related to allyl carbons at 132.6 ($CH_2{=}CH{-}CH_2{-}$), 118.9 ($CH_2{=}CH{-}CH_2{-}$) and 66.0 ppm ($CH_2{=}CH{-}CH_2{-}$), at 42.3 and 23.4 ppm connected to the $-C(CH_3)_2-$ residue, along with a resonance at 59.3 ppm related to the quaternary carbon atom bonded to the Br end-group. These evidences indicate that the allyl groups do not undergo polymerization in the ATRP process. Thus, the knowledge of both the chain end moieties allows to precisely assess, by comparing the integrated allyl NMR signals with respect to those of (*S*)-**MAP** groups, the number average molecular weights $\bar{M}_n$ reported in Table 1, which appear in reasonable agreement with those determined by SEC in the case of poly-3 only, the values found for poly-2 and -1 resulting increasingly divergent. This discrepancy may be attributed to the use of monodispersed polystyrene standards unsuitable to an accurate determination by SEC of the samples having the lowest values of molecular weight. However the difference between the values determined by SEC and NMR appears to decrease upon increasing $\bar{M}_n$ and the values found by SEC for poly-4 through poly-6 can be considered confidently as representative of the actual molecular mass, although they could not be matched with the corresponding values determined by NMR, as this technique could not be adopted for poly-4 to -6 due to the too low relative intensity of the end groups resonances in these samples.

Fig. 3 shows an approximately linear dependence of $\ln([M]_0/[M]_t)$ with time (where, $[M]_0$ and $[M]_t$ are the initial and at t time monomer concentration, respectively), thus indicating a first-order kinetics of the polymerization rate with respect to the monomer concentration and a relatively constant concentration of the growing species throughout the process. Yields and number average molecular weight values of the obtained polymers (Table 1) show a strong dependence on the reaction duration: by varying this last parameter only, we have obtained several samples of various average chain length, as shown by SEC chromatograms reported in Fig. 4. Although a certain closeness to the column exclusion limit may be apparent for the samples with higher molecular mass, the use of two different

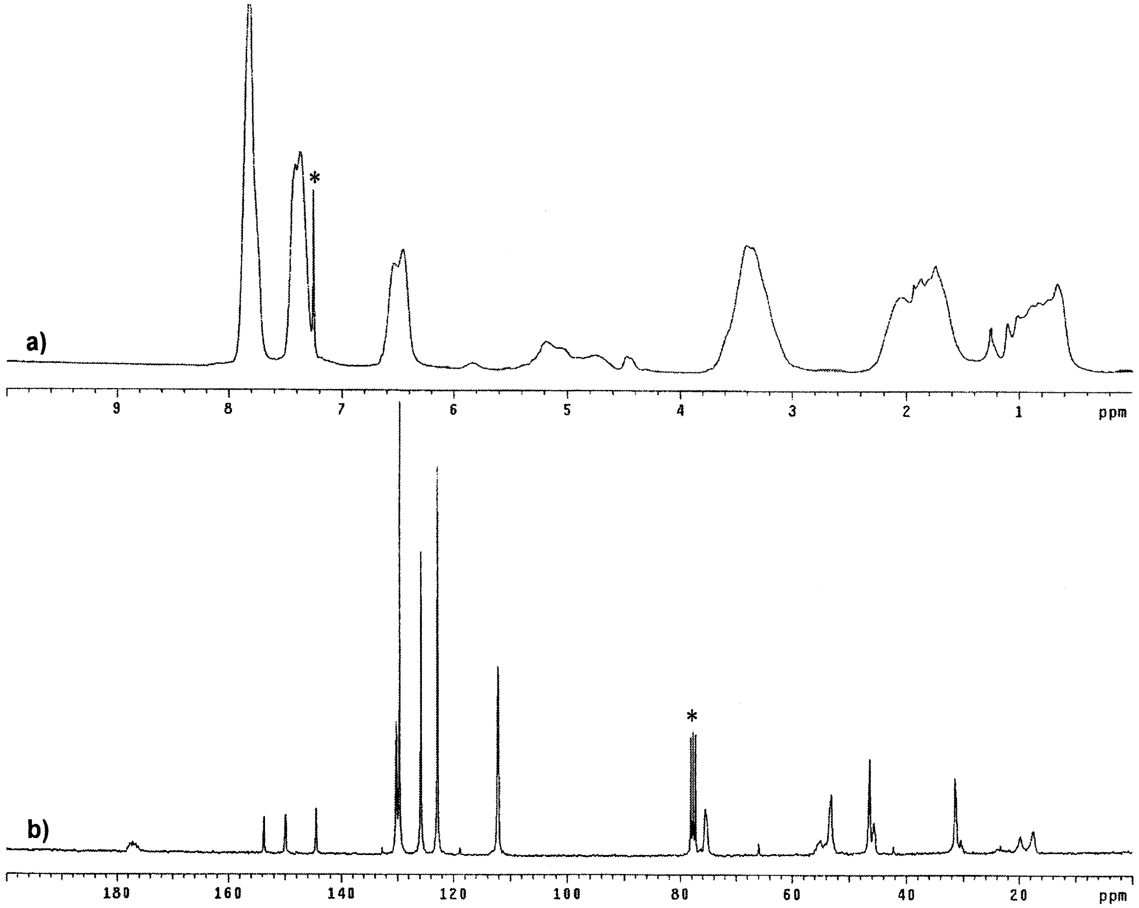

Fig. 2. ^{1}H-NMR (a) and ^{13}C-NMR (b) spectra in $CDCl_3$ of poly-2. Starred signals refer to solvent resonances.

chromatographic columns (see Experimental section) for this determination reasonably confirms that a steady increment of the average molecular weight with time takes place. In addition, a linear correlation between number average molecular weights, determined by SEC and NMR, and monomer conversion (Fig. 5), indicative of the living character of the polymerization, is observed.

Under the same experimental conditions Zhu et al. [23] obtained poly[2-(dimethylamino)ethylmetacrylate] with high yield and high $\bar{M}_n$ in one hour. Similar results have been also reported in Matyjaszewski's review paper [11] for several methacrylic monomers. In our experiments, carried out at 60 °C as the polymerization temperature, and at the same monomer and initiating system concentrations as in

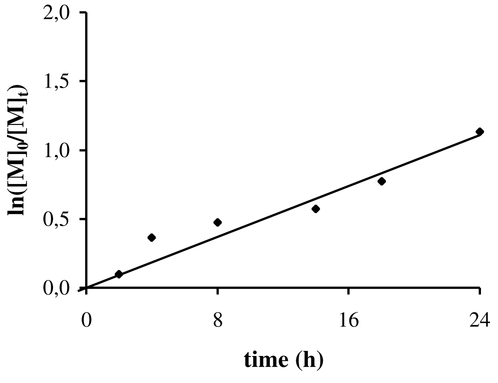

Fig. 3. First order kinetic plot of $\ln([M]_0/[M]_t)$ versus time for the ATRP of (*S*)-**MAP** in THF as solvent [(*S*)-**MAP**/THF 1/20 g/ml] at 60 °C. [(*S*)-**MAP**]:[**ABIB**]:[**HMTETA**]:[CuBr] = 50:1:1:1 by mol.

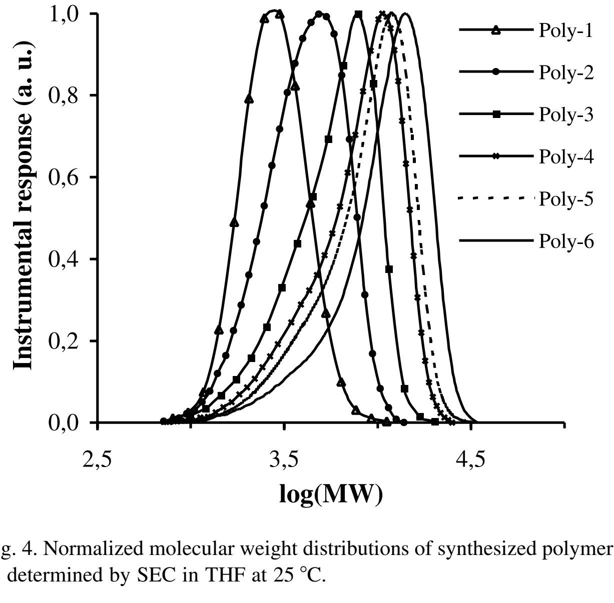

Fig. 4. Normalized molecular weight distributions of synthesized polymers as determined by SEC in THF at 25 °C.

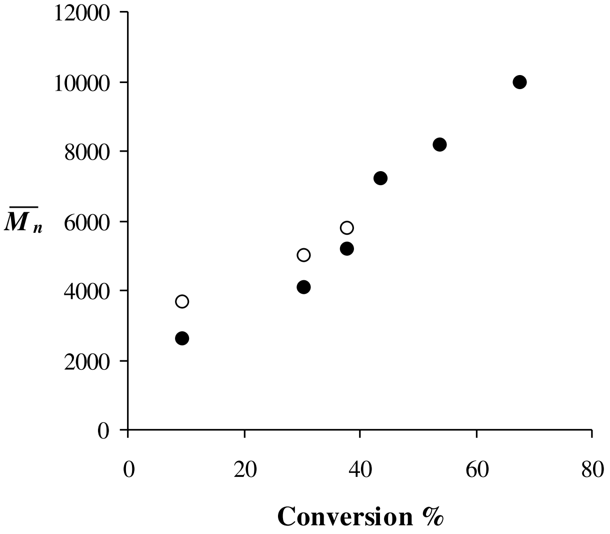

Fig. 5. Evolution of the average molecular weight determined by SEC (●) and NMR (○) versus conversion for the ATRP of (*S*)-**MAP** in THF. Same conditions as in Figure 3.

the above reference [23], we observe a lower polymerization rate and appreciably larger polydispersity indexes (1.2–1.4), with respect to those typical for ATRP (1.1–1.2). This can be ascribed to the well known [1,2,25] low reactivity in the free-radical polymerization of unsatured monomers bearing an azoaromatic group, which is likely to involve the occurrence of chain transfer reactions widening the molecular mass distribution of the macromolecules and in particular increasing the amount of the low molecular weight fraction upon increasing the reaction duration, as evidenced in Fig. 4.

With the aim to study the dependence of the optical activity on the average molecular weight of these materials, the specific $\{[\alpha]_D^{25}\}$ and molar $\{[\Phi]_D^{25}\}$ optical rotation of the polymeric derivatives have been determined. As shown in Table 2, all polymeric products display an optical activity higher than the model compound (*S*)-**PAP** and increasing with the average chain length up to the value for poly[(*S*)-**MAP**], possessing the highest molecular mass in the series. It can be noticed, however, that the optical rotations of poly-6 and poly[(*S*)-**MAP**] are rather close to each other, whereas their number average polymerization degrees $\bar{X}_n$ are very different (about 30 and 94, respectively), thus indicating a flattening of the increase of optical rotation with the macromolecular chain length above values of molecular weight over 10,000 g/mol, even if the higher polydispersity of poly[(*S*)-**MAP**] with respect to poly-6 (1.6 vs. 1.4), contributing presumably to reduce somewhat the optical rotation value of the former derivative, has to be taken into account.

These findings suggest that a remarkable contribution to optical activity by the macromolecular chains is present, which could be attributed in principle to conformational and/or configurational effects originated by a prevalent tacticity of the polymeric backbone.

An evaluation of the microtacticity of all the polymeric derivatives has been made based on the ^{13}C-NMR signals of the methacrylic methyl group, which displays two resonances located at ≈19.8 and 17.5 ppm, assigned to *mr* (meso-racemo) and *rr* (racemo-racemo) heterotactic and syndiotactic triads, respectively [26]. Assuming that the polymerization process follows a Bernoullian statistics, the probabilities of formation of a meso dyad *m* (P_m) can be calculated from the integrated signals ratio (*mr*/*rr*), which corresponds to $2P_m(1-P_m)/(1-P_m)^2$, i.e. to the ratio between the probability of formation of *mr* and *rr* triads [3]. The results for the series of investigated polymers, reported in Table 3 ($P_m = 0.25–0.29$), are quite close to those obtained for poly[(*S*)-**MAP**] [1] prepared by AIBN free radical polymerization ($P_m = 0.26$) and for analogous polymethacrylic derivatives [27], and confirm that the process follows a Bernoullian statistics, as indicated by the similarity of $P_{m/r}$ with $P_{m/m}$ and of $P_{r/m}$ with $P_{r/r}$ (Table 3), as well as by the sum equal to one of $P_{m/r}$ with $P_{r/r}$ and of $P_{m/m}$ with $P_{r/m}$ [28].

Table 2
Specific optical rotation, molar optical rotation and UV–Vis spectra of (*S*)-**PAP** and polymeric derivatives in $CHCl_3$ solution at 25 °C

Samples	$[\alpha]_D^{25}$ [a]	$[\Phi]_D^{25}$ [b]	1st UV–Vis band		2nd UV–Vis band	
			λ_{max} [c]	$\varepsilon_{max} \times 10^{-3}$ [d]	λ_{max} [c]	$\varepsilon_{max} \times 10^{-3}$ [d]
(*S*)-**PAP** [e]	+4.0	+14.0	409	29.8	258	11.6
Poly[(*S*)-**MAP**] [e]	+410	+1374	408	28.3	258	10.5
Poly-1	+130	+435	408	26.4	260	10.6
Poly-2	+312	+1047	408	26.3	257	10.7
Poly-3	+363	+1218	409	25.4	257	11.0
Poly-4	+383	+1284	407	26.7	258	10.6
Poly-5	+383	+1286	409	26.0	259	10.7
Poly-6	+428	+1434	408	26.8	258	10.5

[a] Specific optical rotation, expressed as deg dm^{-1} g^{-1} cm^3.

[b] Molar optical rotation, expressed as deg dm^{-1} mol^{-1} dL and calculated as ($[\alpha]_D^{25}$ *M*/100), where *M* represents the molecular weight of (*S*)-**PAP** or the molecular weight of the repeating unit of poly[(*S*)-**MAP**].

[c] Wavelength of maximum absorbance, expressed in nm.

[d] Expressed in L mol^{-1} cm^{-1} and calculated for one single chromophore.

[e] Ref. [1].

Table 3
Microtacticity of polymeric derivatives as determined by ^{13}C-NMR

Polymers	P_m	P_r	mm (%)	mr(rm) (%)	rr (%)	$P_{m/r}$	$P_{r/m}$	$P_{m/m}$	$P_{r/r}$
Poly-1	0.27	0.73	7	39	54	0.27	0.73	0.27	0.73
Poly-2	0.29	0.71	8	41	51	0.29	0.71	0.29	0.71
Poly-3	0.25	0.75	6	38	56	0.25	0.75	0.25	0.75
Poly-4	0.29	0.71	9	41	50	0.29	0.71	0.29	0.71
Poly-5	0.27	0.73	7	39	54	0.27	0.73	0.27	0.73
Poly-6	0.26	0.74	7	39	55	0.26	0.74	0.26	0.74
Poly[(*S*)-**MAP**][a]	0.26	0.74	7	38	55	0.26	0.73	0.27	0.74

P_m and P_r represent the probability of formation of *meso* and *racemo* dyads; *mm*, *mr*(*rm*) and *rr* are the percent amounts of triads present in the polymers; $P_{m/r}$, $P_{r/m}$, $P_{m/m}$ and $P_{r/r}$ are the calculated probabilities that a given dyad follows a dyad having the same or the opposite relative configuration.

[a] Ref. [1].

Thus, the main chain microstructure is essentially atactic, with a predominance of syndiotactic triads ($rr=50$–56%) suggesting a substantially low stereoregularity of the main-chain. This behaviour confirms that the ATRP of monomer (*S*)-**MAP** is poorly stereoselective, to a similar extent as the AIBN-initiated polymerization, and hence is unable to favour a strongly predominant tacticity of the macromolecules. The high values of optical activity observed are therefore to be attributed to the assumption by the macromolecules in solution of dissymmetric conformations of one prevailing chirality to an extent related to their average chain length.

3.2. Thermal properties

The decomposition temperatures of all polymeric samples (around 300 °C), determined by thermogravimetric analysis, are significantly high, due to the presence of strong dipolar interactions between azobenzene chromophores in the side chain. The DSC thermograms (Table 1) exhibit only second order thermal transitions related to glass transitions, the T_g values of poly-1 to -6 increasing from 122 to 160 °C (Table 1), thus approaching the maximum value of 169 °C found for poly[(*S*)-**MAP**] [1], obtained by AIBN-initiated free radical polymerization. As expected, the increase of the average molecular weight appears to strongly reduce the mobility of polymeric chains as a consequence of the increased extent of interchromophore interactions. Observation of the polymeric samples with a polarising microscope did not reveal any liquid crystalline behaviour, in accordance with the amorphous character of these polymers, at least at microscopic level.

Both the good thermal stability and high values of T_g suggest that these polymeric systems, although possessing a low average molecular weight, may be promising for solid state applications in optoelectronics due to their stability at room temperature subsequently to photo- or electrically induced orientation of the azoaromatic dipoles.

3.3. UV-vis properties

The UV–Vis spectra of all polymeric derivatives in $CHCl_3$ solution (Table 2) exhibit in the 250–700 nm spectral region two absorption bands, centred around 408 and 258 nm. The former one, more intense, is attributed to electronic transitions such as n-π^*, π–π^* and internal charge transfer of the azobenzene chromophore. The latter to the π–π^* electronic transition of aromatic ring [25].

A significant hypochromism was formerly observed for both the first and the second band when passing from the model (*S*)-PAP to the corresponding polymer poly[(*S*)-MAP] [1], regardless the solvent employed. Similar behaviour was previously reported for several polymers bearing side-chain aromatic chromophores [29–31] and attributed to the occurrence of electrostatic dipole-dipole interactions between the neighbouring aromatic chromophores [32–34]. These are short range interactions occurring between dipoles linked to the same (intra-chain interactions) or to different macromolecular chains (inter-chain interactions), the former being more likely at high dilution of chromophores ($c \approx 3\times10^{-4}$ M), in the conditions at which the UV spectra have been recorded. As shown in Table 2, the molar absorption coefficient values related to the first absorption band are in the range 25.4–26.8×10^{-3} L mol^{-1} cm^{-1} for poly-1 through poly-6, with no apparent dependence on the average polymerization degree of the samples examined, all these values resulting lower than those observed in the model compound (*S*)-PAP and even in poly[(*S*)-MAP] having $\bar{M}_n = 31500$ g/mol.

3.4. CD spectra and chiroptical properties

In order to evidence the existence of dissymmetric conformations of the macromolecules in solution, the series of polymeric derivatives poly-1 to -6 has been characterized by CD in chloroform solution in the spectral region between 250 and 700 nm, and the spectra obtained have been compared with those carried out [1] under the same conditions for poly[(*S*)-**MAP**] and (*S*)-**PAP** (Table 4 and Fig. 6).

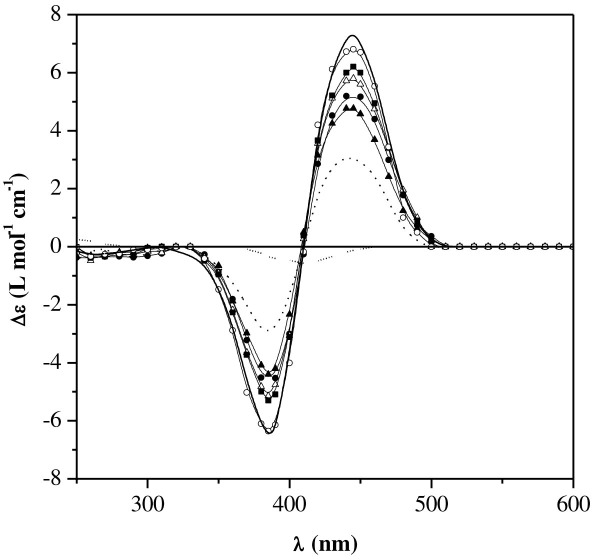

Fig. 6. CD spectra of poly-1 (···), poly-2 (-▲-), poly-3 (-●-), poly-4 (-△-), poly-5 (-■-), poly-6 (-○-) as compared to (*S*)-**PAP** (- - -) and poly[(*S*)-**MAP**] (—).

All samples of poly-1 to -6 display two intense dichroic bands of opposite sign and slightly different intensity in correspondence of the first UV-vis absorption band, with a crossover point close to 408–410 nm, the wavelength of maximum absorption. Such a behaviour is typical of exciton splitting originated by cooperative interactions between side-chain azoaromatic chromophores disposed according to a mutual chiral geometry of one prevailing handedness [1, 35]. By contrast, the CD spectrum of model (*S*)-**PAP** displays only two weak bands at 410 and 258 nm, related to the UV–Vis absorptions, indicative of the absence of the above interactions as a consequence of the lack of any structural restriction. It is to be noted that the CD spectra of poly-1 to -6 display increasing amplitudes upon increasing the average molecular weight up to a value very close to that shown by poly[(*S*)-**MAP**], in agreement with the results obtained by polarimetry, as shown in Fig. 7, reporting the integrated areas of the dichroic bands connected to the first UV–Vis absorption band as a function of the average number polymerization degree.

The amount of dissymmetric conformations assumed by the macromolecules in chloroform solution appears strongly dependent on their molecular mass, their extent reaching a maximum value roughly corresponding to a $\bar{X}_n$ value of 30, after which it remains approximately constant. It appears therefore that the presence of side-chain chromophores possessing a prevailing helicity is initially affected by the vicinity of mobile chain ends limiting their formation, this effect being progressively reduced with the increase of the chain length. At a sufficiently high value of the molecular mass, however, their overall amount does not furtherly change, since it is probably determined by their thermodynamical stability under the experimental conditions adopted (solvent, temperature etc.).

Table 4
CD spectra in $CHCl_3$ solution at 25 °C

Samples	1st absorption band					2nd absorption band	
	λ_1[a]	$\Delta\varepsilon_1$[b]	λ_0[c]	λ_2[a]	$\Delta\varepsilon_2$[b]	λ_3[a]	$\Delta\varepsilon_3$[b]
(*S*)-**PAP**	410	−0.51	–	–	–	258	+0.22
Poly-1	441	+3.05	410	384	−2.96	258	−0.28
Poly-2	443	+4.76	408	385	−4.29	258	−0.34
Poly-3	444	+5.15	411	386	−4.49	258	−0.34
Poly-4	444	+5.79	409	385	−5.01	259	−0.41
Poly-5	445	+6.10	409	386	−5.21	260	−0.42
Poly-6	445	+6.79	409	386	−6.36	260	−0.44
Poly[(*S*)-**MAP**][d]	445	+7.35	409	387	−6.42	258	−0.32

[a] Wavelength (in nm) of maximum dichroic absorption.
[b] Δε expressed in L mol^{-1} cm^{-1} and calculated for one repeating unit in the polymer.
[c] Wavelength (in nm) of the cross-over of dichroic bands.
[d] Ref. [1]

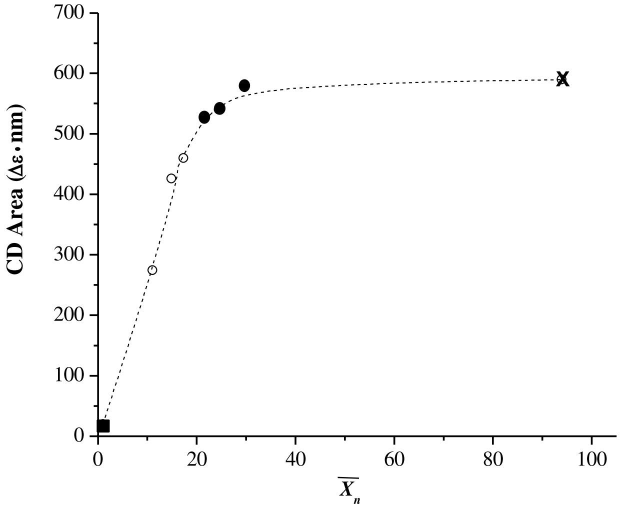

Fig. 7. Evolution of the amplitude of the CD exciton couplet with the average number polymerization degree as determined by SEC (●) and ^{1}H-NMR (○). The values for (*S*)-**PAP** (■) and poly[(*S*)-**MAP**] (**X**) are also reported.

4. Conclusions

A series of optically active photochromic methacrylic polymers has been synthesized for the first time by ATRP starting from the corresponding monomer. Several homopolymers having various average molecular weight and low polydispersity index have been obtained just changing the reaction duration.

The optical activity of all the polymeric derivatives results to be much higher that those of monomer and low molecular weight model compound and increases with increasing the average molecular weight. The results indicate that the chirality of these macromolecules is due to conformational effects and strongly depends on the chain length up to a maximum limit after which it does not increase further.

The glass transition temperatures of these materials are related to the average molecular weight, reaching values as high as 160 °C. These high values are due to the presence of strong polar interactions between chromophores in the solid state, and appear promising for application in micro- and opto-electronics. As assessed by NMR, each macromolecular chain contains two reactive end-groups, i.e. allyl and bromide, which could furtherly be used to obtain various derivatives by standard organic procedures. The living nature of the radical process therefore suggests that these photochromic optically active homopolymers could be employed to prepare novel block copolymers, even of complex architecture (star polymers, etc.), with interesting properties and potential applications in advanced technologies.

Acknowledgements

The financial support by MIUR (Fondi FIRB 2001 and PRIN 2004) and Consorzio INSTM is gratefully acknowledged.

References

[1] Angiolini L, Caretti D, Giorgini L, Salatelli E. J Polym Sci, Part A: Polym Chem 1999;37:3257.
[2] Angiolini L, Caretti D, Giorgini L, Salatelli E. Macromol Chem Phys 2000;201:533.
[3] Angiolini L, Caretti D, Giorgini L, Salatelli E. Polymer 2001;42:4005.
[4] Carlini C, Angiolini L, Caretti D. Photocromic optically active polymers. In: Polymeric materials encyclopedia, vol.7. Boca Raton: CRC Press; 1996. p. 5116.
[5] Proceedings of the Symposium on Azobenzene-Containing Materials, Boston MA (USA) 1998, ed. A Natansohn, Macromolecular Symposia 137, 1999. p.1–165.
[6] Verbiest T, Kauranen M, Persoons A. J Mater Chem 1999;9:2005.
[7] Hopkins TE, Wagener KB. Adv Mater 2002;14:1703.
[8] Xie S, Natanshon A, Rochon P. Chem Mater 1995;5:403.
[9] Angiolini L, Bozio R, Giorgini L, Pedron D, Turco G, Daurù A. Chem Eur J 2002;8:4241.
[10] Angiolini L, Benelli T, Bozio R, Daurù A, Giorgini L, Pedron D. Sinth Met 2003;139:743.
[11] Coessens V, Pintauer T, Matyjaszewski K. Prog Polym Sci 2001;26:337.
[12] Percek V, Barboiu B, Kim HJ. J Am Chem Soc 1998;120:305.
[13] Gaynor S, Qiu J, Matyjaszewski K. Macromolecules 1998;31:5951.
[14] Ibrahim K, Lofgren B, Seppala J. Eur Polym J 2003;39(5):939–44.
[15] Xia J, Johonson T, Gaynor S, Matyjaszewski K, DeSimone J. Macromolecules 1999;32:4802.
[16] Zhang Z, Ying S, Shi Z. Polymer 1999;40:5439.
[17] Demirelli K, Kurt A, Coskun M. Eur Polym J 2004;40:451.
[18] He X, Zhang H, Wang X. Polym J 2002;34:523.
[19] Wang X, Zhang H, Zhong G, Wang X. Polymer 2004;45:3637.
[20] He X, Yan D, Mai Y. Eur Polym J 2004;40:1759.
[21] Wang J-S, Matyjaszewski K. J Am Chem Soc 1995;117:5614.
[22] Patten TE, Xia J, Abernathy T, Matyjaszewski K. Science 1996;272:866.
[23] Zeng F, Shen Y, Zhu S, Pelton R. Macromolecules 2000;33:1628.
[24] Perrin DD, Amarego WLF, Perrin DR. Purification of laboratory chemicals. Oxford: Pergamon Press; 1966.
[25] Altomare A, Ciardelli F, Ghiloni MS, Solaro R, Tirelli N. Macromol Chem Phys 1997;198:1739.
[26] Peat IR, Reynolds WF. Tetrahedron Lett 1972;1359.
[27] Angiolini L, Caretti D, Giorgini L, Salatelli E, Altomare A, Carlini C, Solaro R. Polymer 1998;39:6621.
[28] McCord E, Anton WL, Wilczek L, Ittel SD, Nelson LTJ, Raffell KD. Macromol Symp 1994;86:47.
[29] Chiellini E, Solaro R, Galli G, Ledwith A. Macromolecules 1980;13:1654.
[30] Majumdar RN, Carlini C. Makromol Chem 1980;181:201.
[31] Carlini C, Gurzoni F. Polymer 1983;24:101.
[32] Tinoco Jr I. J Am Chem Soc 1960;82:4785.
[33] Okamoto K, Itaya A, Kusabayashi S. Chem Lett 1974;1167.
[34] Ciardelli F, Aglietto M, Carlini C, Chiellini E, Solaro R. Pure Appl Chem 1982;54:521.
[35] Ciardelli F, Carlini C, Solaro R, Altomare A, Pieroni O, Houben JL. Fissi A Pure Appl Chem 1984;56:329.